ACADEMIA ROMÂNĂ
Revue Roumaine de Chimie
https://www.icf.ro/rrch/

Rev. Roum. Chim.,
2022, *67*(1-2), 51–62
DOI: 10.33224/rrch.2022.67.1-2.03

Dedicated to the memory of
Dr. Emilian GEORGESCU (1946-2020)

PHOTOPHYSICAL AND BIOLOGICAL PROPERTIES OF A STRIGOLACTONE MIMIC DERIVED FROM 1,8-NAPHTHALIC ANHYDRIDE

Ioana BALA,[a,b] Anton AIRINEI,[c] Emilian GEORGESCU,[d] Florin OANCEA,[a,b,*] Florentina GEORGESCU,[e] Alina NICOLESCU,[c,f,*] Radu TIGOIANU[c] and Calin DELEANU [c,f,*]

[a] National Research & Development Institute for Chemistry & Petrochemistry – ICECHIM, Spl. Independenţei 202, RO-060021 Bucharest, Roumania
[b] University of Agronomic Sciences and Veterinary Medicine of Bucharest, Blvd. Mărăşti 54 RO-011464 Bucharest, Roumania
[c] "Petru Poni" Institute of Macromolecular Chemistry, Roumanian Academy, Aleea Grigore Ghica Voda 41-A, RO-700487 Iaşi, Roumania
[d] Chimcomplex Research Center, St. Uzinei 1, RO-240050 Râmnicu Vâlcea, Roumania
[e] Enpro Soctech Com srl, Str. Elefterie 51, RO-050524 Bucharest, Roumania
[f] "Costin D. Nenitzescu" Institute of Organic and Supramolecular Chemistry, Roumanian Academy, Spl. Independenţei 202-B, RO-060023 Bucharest, Roumania

Received October 15, 2021

The paper presents the spectroscopic and biological properties the 2-(4-methyl-5-oxo-2,5-dihydro-furan-2-yloxy)-benzo[*de*]isoquinoline-1,3-dione, a strigolactone mimic derived from 1,8-naphthalic anhydride. This compound presents fluorescent properties and has interesting effects on biofilm formation by nodulation enhancer bacteria. The results demonstrate the possibility to prepare novel fluorescent compounds as strigolactones-like activities in order to be exploited in bioimaging studies.

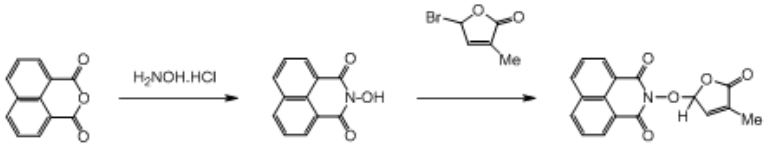

INTRODUCTION

Strigolactones (SLs) are naturally carotenoid derivatives, released by plants into the soil as communication signal. Strigol, the first member of this group of compounds identified as potent germination stimulants of parasitic weed seeds,[1,2] gave the generic name of this class of compounds. SLs act as signaling molecules for the germination of seed of parasitic weeds,[1-7] and forhyphal branching in arbuscularmycorrhizal (AM) fungi.[8-11] SLs are active phytohormones in controlling the architecture of various plant organs,[11-19] and play an important role in plants responses to both biotic and abiotic stresses.[20-24] More than 25 naturally occurring SLs have been identified so far in the root exudates of several plant species. This group of compounds share a tricyclic lactone (ABC rings) linked *via* an enol-ether bond to an invariable α,β-unsaturated furanone moiety labeled as D ring.[25,26] They are grouped into two families with different stereochemistry: one with the parent structure of strigol and the other with the parent structure of oronbachol (Figure 1).

The structure-activity relation studies on SLs shown that the bioactiphore CD part, the stereochemistry and the methyl substituent at C-4′ of the D-ring are essential requirements for SLs activity as germination stimulants for the seeds of parasitic

* Corresponding authors: florin@ping.ro (F.O.); alina220382@yahoo.com (A.N.); calin.deleanu@yahoo.com (C.D.)

weeds.[7,27] SLs bioactivity is not affected by the structural changes of A, B and even C rings or by the replacement of an oxygen atom by a nitrogen atom[28,29] or a sulfur atom.[18] Instead, the presence of ABC rings and the stereochemistry seem to be essential for proliferation of AM fungi hyphae.[11,30,31]

Naturally occurring SLs have too complex structures for multi-gram scale syntheses and have been isolated from plant roots exudates only in very small amounts. As a consequence, compounds with simplified structures of SL analogs and mimics have been designed and prepared in order to understand their various structure-relationship activities and to identify the corresponding receptors in plants. The SL analogs retain the bioactiphore CD part of natural SLs and have an extensive structural freedom in the AB-rings of the molecule (Figure 2).[32-38]

SL mimics in which the bioactive D-ring is directly linked to (hetero)aryloxy, aroyloxy, arylthio or (hetero)aromatic moieties mimic a variety of biological activities of natural SLs, even without the typical structural features of natural SLs (Figure 3).[39-45]

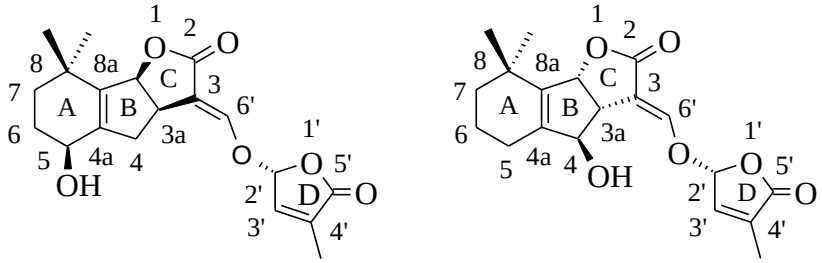

Fig. 1 – The structure of parent compounds for the two major groups of naturally SLs.

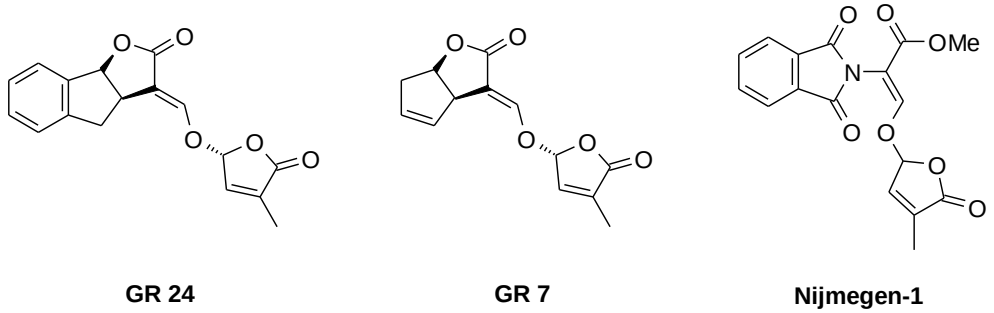

Fig. 2 – Chemical structures of several strigolactone analogs.

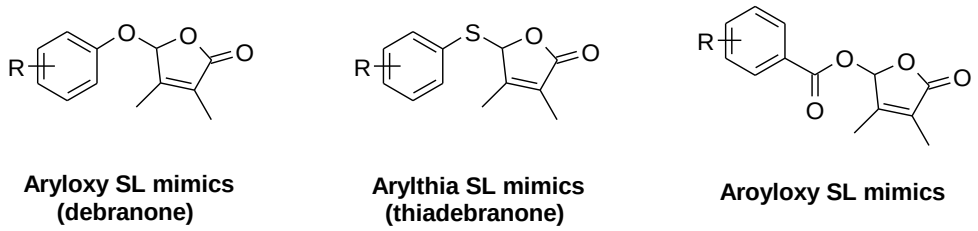

Fig. 3 – General structures of some strigolactone mimics.

Following our previous researches on bioactive compounds,[45-48] we have been interested in synthesis and properties of new active compounds for plant protection. Consequently, we have synthesized novel SL mimics, including an SL mimic bearing the 1,8-naphthalimide system, namely 2-(4-methyl-5-oxo-2,5-dihydro-furan-2-yloxy)-benzo[*de*]isoquinoline-1,3-dione, starting from 2-hydroxy-1,8-naphthalimide and 5-bromo-3-methyl-furan-2-one.[45] We demonstrated the effect of this new strigolactone mimic on parasitic seed germination and fungal pathogens development pattern.[45] Now, we report here a more efficient synthetic procedure for multi-grams synthesis of this SL mimic which contain in its molecule the 1,8-naphthalimide ring connected by an ether link to the bioactive 3-methyl-furan-2-one unit, as well as its interesting fluorescent and biological properties, i.e. promotion of biofilm formation by a nodulation enhancer bacteria.

RESULTS AND DISSCUSION

Synthesis and photophysical properties of SL mimic 4

The efficient synthetic procedure for the synthesis of 2-(4-methyl-5-oxo-2,5-dihydrofuran-2-yloxy)-benzo[*de*]isoquinoline-1,3-dione (SL mimic **4**, synonym with 3-methyl-5-(benzo[*de*]isoquinoline-1,3-dione-2-yloxy)-5*H*-furan-2-one) starts from cheap, commercially available, 1,8-naphthalic anhydride **1**. By treating 1,8-naphthalic anhydride with hydroxylamine hydrochloride in dioxane, under basic conditions, 2-hydroxy-1,8-naphthalimide (**2**) was easily obtained in very good yield. The intermediate 5-bromo-3-methylfuran-2-one (**3**) was obtained in good yield by the bromination of 3-methyl-5*H*-furan-2-one with *N*-bromosuccinimide in CCl_4, in the presence of benzoyl peroxide,[49] and was used after the removal of the solvent as crude reaction product, without purification. In the last step, 2-hydroxy-1,8-naphthalimide (**2**) was coupled with 5-bromo-3-methyl-furan-2-one (**3**) in DMF in the presence of anhydrous potassium carbonate to access the desired SL mimic **4** in good yield and in multi-gram amounts (Scheme 1).

The chemical structure of SL mimic **4** was confirmed by chemical, IR and NMR analyses.[45] Thus, the NMR signals present in the proton and carbon spectra of SL mimic 4 resonate mainly in the downfield region, in accordance with the proposed chemical structure. Except the methyl signals, that were straightforward identified, the rest of the signals were assigned based on the correlations obtained in the 2D spectra like H-C HSQC and H-C HMBC. Because CH groups' signals were well resolved and separated in both proton and carbon spectra, the assignments were obtained from the standard proton-carbon direct bond correlations. The quaternary carbons from the structure were differentiated based on their three-bond couplings with the neighboring protons, present in the H-C HMBC spectrum. In the case of quaternary carbons C-6'a and C-9'b, the resolution obtained in the classical H-C HMBC experiment was not good enough to distinguish between the correlation signals. These two carbons were assigned after recording a higher resolution version of the H-C HMBC experiment with shaped pulses that allows acquisition on smaller spectral regions, around the signals of interests. In this experiment (Figure 4), a pulse with specific shapes, different from the classical rectangle, is used to selectively excite the region of interest. The result is a 2D spectrum with a better resolution, thus a better separation between the correlation signals, as it can be seen in Figure 1.

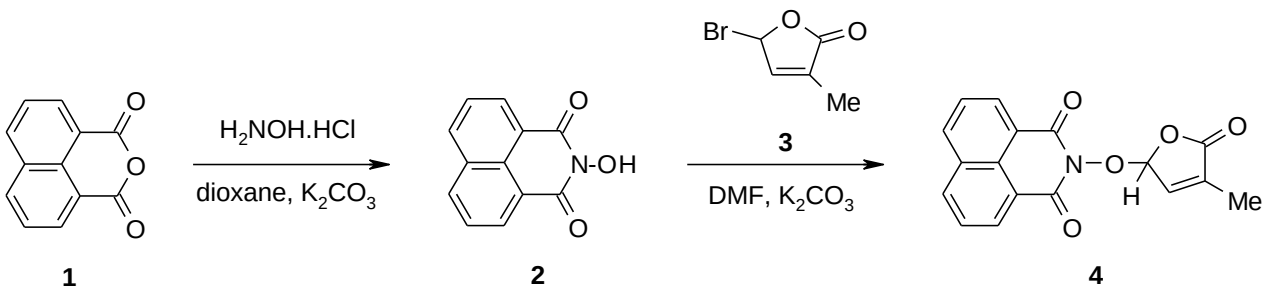

1 **2** **4**

Scheme 1 – An efficient synthesis of the SL mimic **4**.

Besides the specific changes in proton and carbon spectra, previously mentioned by us for several strigolactone analogues,[45] the success of the coupling reaction can be determined from the long-range proton-nitrogen correlations as well. Thus, in the H-N HMBC spectrum for SL mimic **4** (Figure 5), it can be noticed a correlation signal between the nitrogen from naphthalimide (223.1 ppm) and the proton H-5 (6.48 ppm) from furan-2-one moiety.

HRMS isotopic pattern (Figure 6) also confirms the structure of SL mimic **4**, in addition to the $[M+Na]^+$ exact monoisotopic mass (332.0518 m/z).

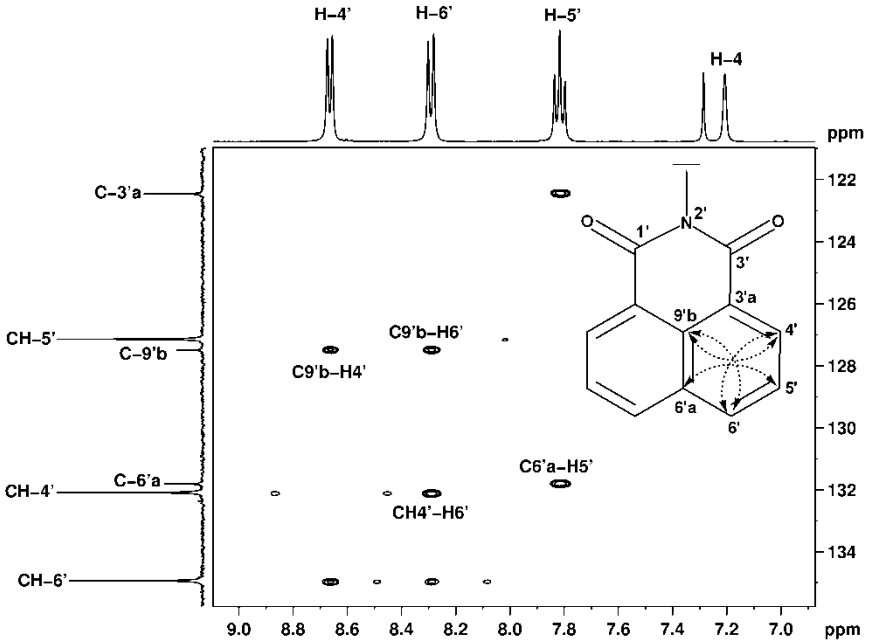

Fig. 4 – Shape pulse H-C HMBC spectrum recorded for SL mimic 4, in $CDCl_3$, at 400 MHz. The correlations of interest are annotated on the 2D plot.

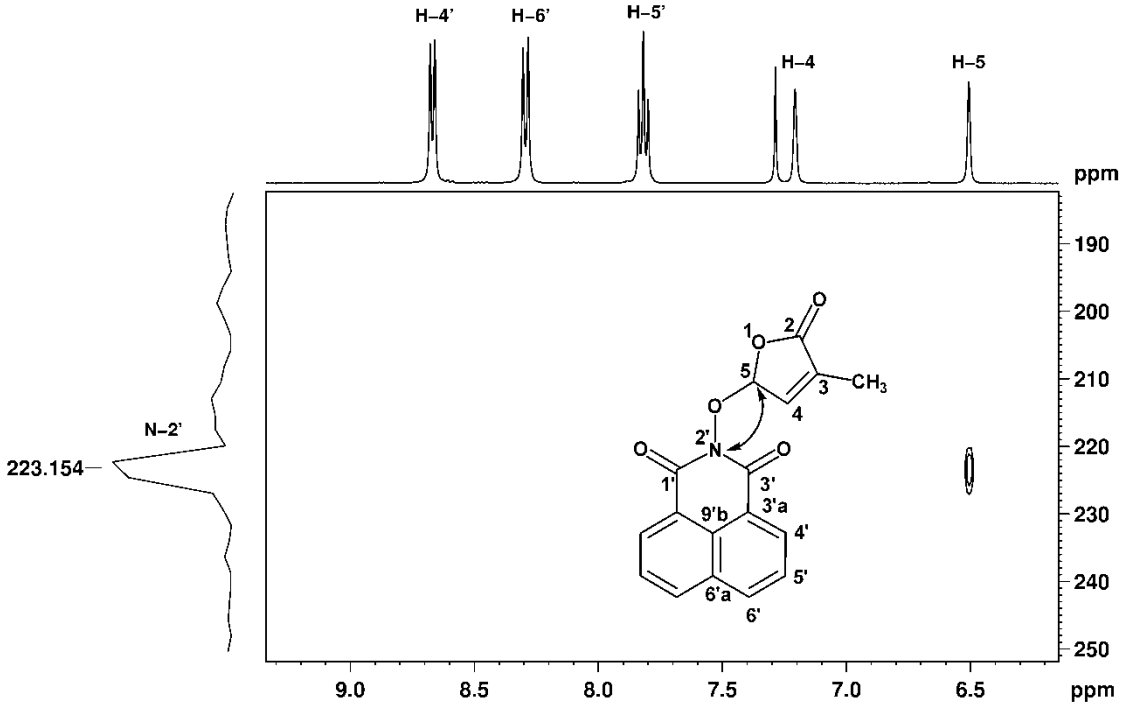

Fig. 5 – H-N HMBC spectrum recorded for SL mimic 4, in $CDCl_3$, proving the success of the coupling reaction.

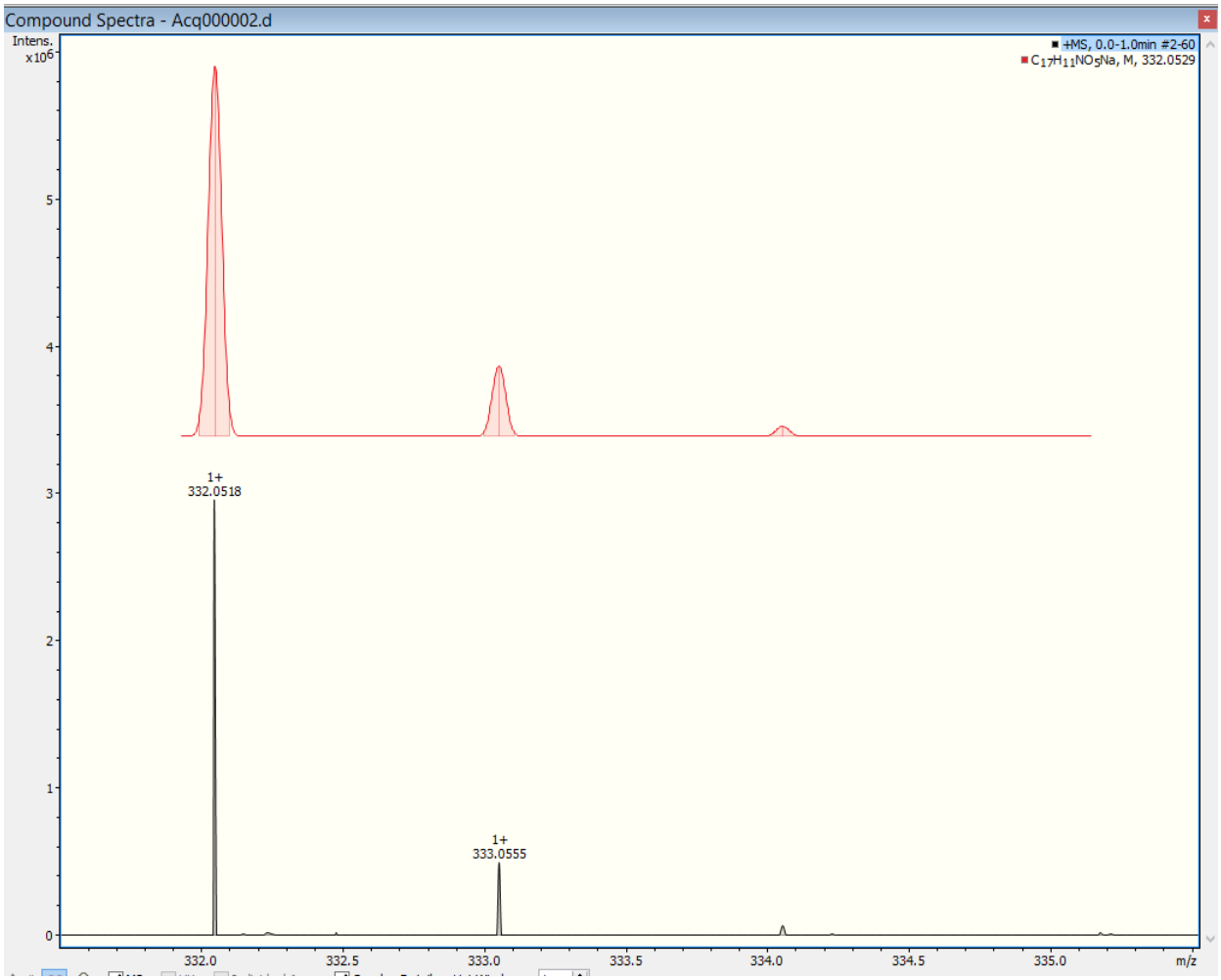

Fig. 6 – HRMS-ESI spectrum with isotopic pattern in positive mode for SL mimic 4. Upper trace (red) – simulated pattern, lower trace (black) – experimental spectrum for $C_{17}H_{11}NO_5Na$ $[M+Na]^+$.

Table 1

Photophysical data of the SL mimic **4** in different organic solvents

Solvent	λ_{abs} (nm)	λ_{em} (nm)	$\Delta\upsilon$ (cm^{-1})	Φ (%)	τ_1 (a_1) (ns; (%))	τ_2 (a_2) (ns; (%))	τ_3 (a_3) (ns; (%))
PhMe	320 sh, 335, 350	403.8	5085	1.86	1.49; (48.44)	5.99; (51.56)	-
$CHCl_3$	325 sh, 337, 351	364, 382, 400 sh	3555	19.21	0.08; (96.19)	1.04; (3.81)	-
DCM	320 sh, 336, 350 sh	362.3, 381, 399.5	3506	25.67	-	-	-
DMF	325 sh, 336, 350 sh	377.7	3284	0.01	0.30; (35.75)	1.26; (35.34)	5.09; (28.91)

During the synthesis we realized that SL mimic **4** showed a luminescent behavior when subjected to UV radiation. A preliminary spectral study of photophysical properties of SL mimic **4** was performed in solvents with different polarities such as toluene (PhMe), chloroform, dichloromethane (DCM) and dimethylformamide (DMF). The photophysical parameters for the SL mimic **4**, namely absorption maxima (λ_{abs}), emission maxima (λ_{em}), Stokes shifts ($\Delta\upsilon$), quantum yield of fluorescence (Φ) and fluorescence lifetimes (τ) in solvents with various polarities are given in Table 1.

The SL mimic **4** presents absorption maxima in the range of 300-375 nm, with a central maximum around 336 nm in DCM, arising from a $\pi\rightarrow\pi^*$ electronic transition of the 1,8-naphthalimide unit. SL mimic **4** shows a violet emission at about 404 nm in toluene. On comparing the emission maxima in a nonpolar solvent with that in a polar solvent, a shift to shorter wavelengths was observed (Table 1). The Stokes shift ($\Delta\upsilon = \upsilon_{abs} - \upsilon_{em}$) and quantum yield of fluorescence (Φ) are important parameters of a fluorescent compound. The Stokes shift reveals the differences in the structure and

properties of fluorophores between ground state and the first excited state. The Stokes shift for SL mimic **4** is in the range 3284-5085 cm^{-1} in solvents with different polarities (Table 1). The SL mimic **4** presents solvent-dependent emission characteristics. While a significant fluorescence was observed in chlorinated solvents, the emission intensity diminished drastically in toluene and DMF. The fluorescence quantum yield was of 19.21% in chloroform and 25.67% in DCM, respectively, while very low values of quantum efficiency were determined in toluene (1.86%) and DMF (0.01%). The fluorescence decay obeys a biexponential law in toluene and chloroform, with a very fast component (0.08 ns and high amplitude of 96.19%) in chloroform. However, the emission decay in DMF was cleanly fitted with a model based on three exponentials. Also, the very fast component was maintained (Table 1).

Since the emission profile of derivative **4** was found to be solvent-dependent, the emission and absorption spectra were investigated in the binary system of DMF/water. The emission spectra of **4** in DMF solution as a function of water content are depicted in Figure 7. Upon exciting at 355 nm, the emission intensity increases with the water content in the range of 0-35%. At the same time, increasing the water content, the emission band underwent a red shift to 395 nm. When the water content increased around 35%, the emission intensity of **4** in DMF/water mixture was 1.3-fold higher than that in pure DMF (Figure 7). The increase of the water content over 35% leads to the decrease of the emission intensity due to a fluorescence quenching process.

The absorption band of **4** was shifted to longer wavelengths as the water content increased (Figure 8). The red shift of emission and absorption maxima can be induced by the increase of mixture polarity as the water content increases. Also, the enhancement in fluorescence and the red shift of the emission and absorption bands can be associated with an aggregation induced emission process in derivative **4**.[50] These data showed interesting fluorescent properties for the SL mimic **4** which contain a fluorophore molecule of 1,8-naphthalimide.

Fluorescent derivatives were developed for cyanoisoindole strigolactone analogs, CISAs,[51] and PL-series of strigolactone analogs.[52] The strigolactone mimic **4** has fluorescent properties that, combined with his proven activity toward rhizosphere organisms and microorganisms, could be used to evaluate the presence of the receptors for SL bioactiphore on the rhizosphere micro-organisms. The advantage of strigolactone mimics is that they are simplified molecules. The most studied plant strigolactone receptors bind and hydrolyze the SL molecules.[53] However, the butenolide part of SL seems to interact with histidine and further stabilize the SL with the transcriptional repressor.[54] Due to its simpler structure, strigolactone mimic **4** could be an effective tool in chasing the SL receptors from rhizosphere microorganisms in bioimaging studies.

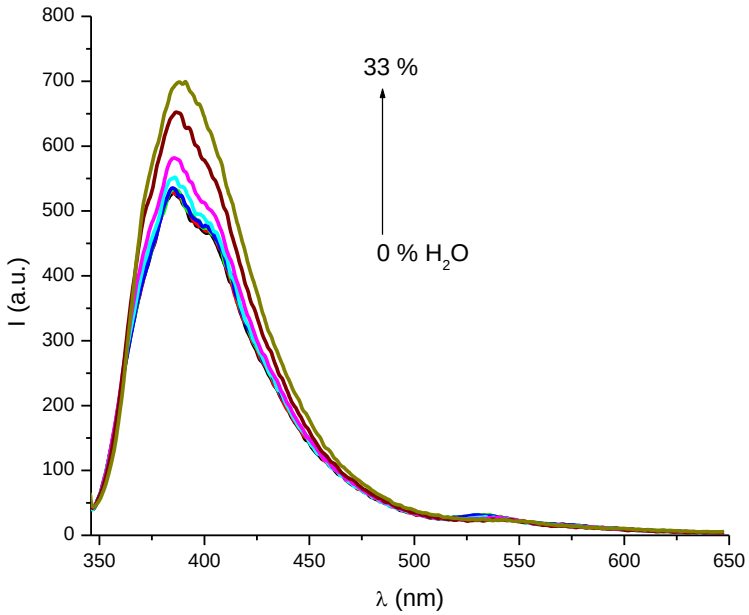

Fig. 7 – The emission spectra of 4 in DMF solution as a function of water content for 335 nm excitation wavelength.

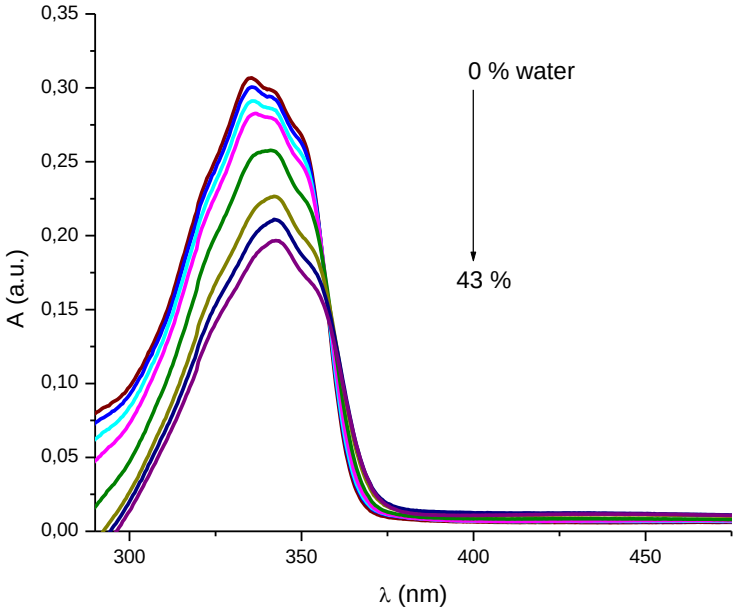

Fig. 8 – The absorption spectra of 4 in DMF/water solutions.

Biological properties of SL mimic 4

The tested GR24 and SL mimic **4** did not have an effect of branching activities of *A. alliaceus* DSM 813 (Figure 9). After 3 days at 28ºC, for the strain *Aspergillus alliaceus*, it can be observed the distribution and the number of the hyphae. The number of hyphae was recorded on a total lengths of 1000 µm, beginning from the end of the youngest hyphal edge. For the straight hyphae one measurement was enough in comparison with curved hyphae where several measurements on linear portions were made to achieve the final length.

In the case of the GR24 treatment with various concentrations (C1 = $5x10^{-6}$, C2 = 10^{-5}, C3 = $5x\ 10^{-5}$ M) it showed that this synthetic strigolactone had no effect of the hyphal branching, and also did not determine the formation of a bigger order of branches compared with those which were present in the controls.

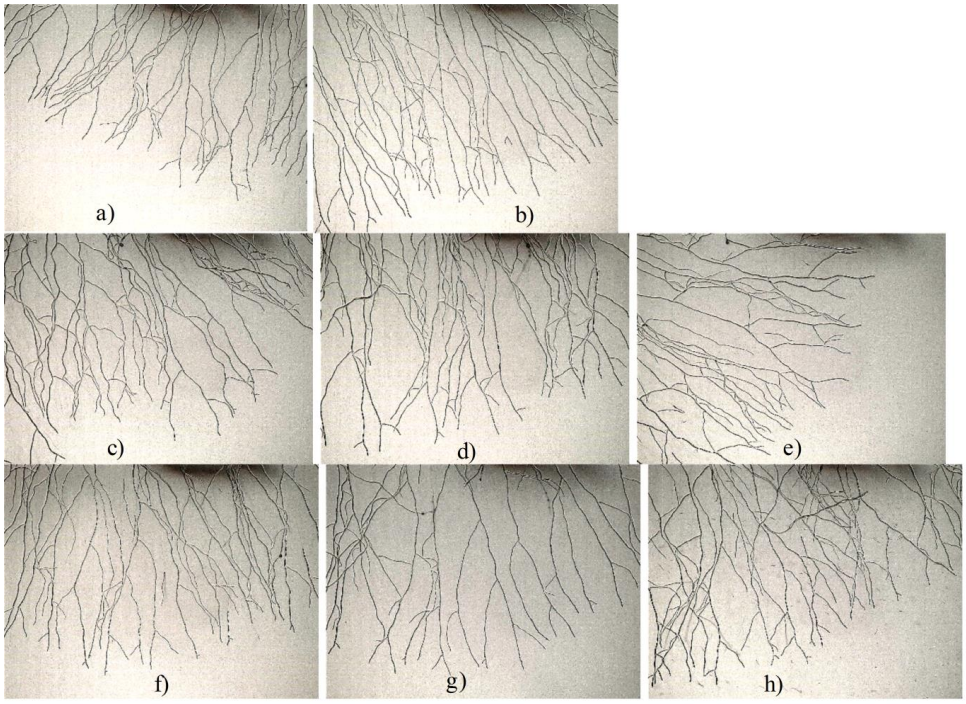

Figure 9 – The aspect of hyphal braching of *Aspergillus alliaceus*in a) control water agar, b) acetone, c) GR24 C1, d) GR24 C2, e) GR24 C3, f) SL **4** C1, g) SL **4** C2, h) SL **4** C3 recorded on a total length of 1000 µm, beginning from the end of the youngest hyphal edge.

Table 2

ANOVA details for the effect of different treatments on the hyphal branches number

	Sum of Squares	df	Mean Square	F	Sig.
Between Groups	1.260	7	0.180	2.609	0.053
Within Groups	1.104	16	0.069		
Total	2.365	23			

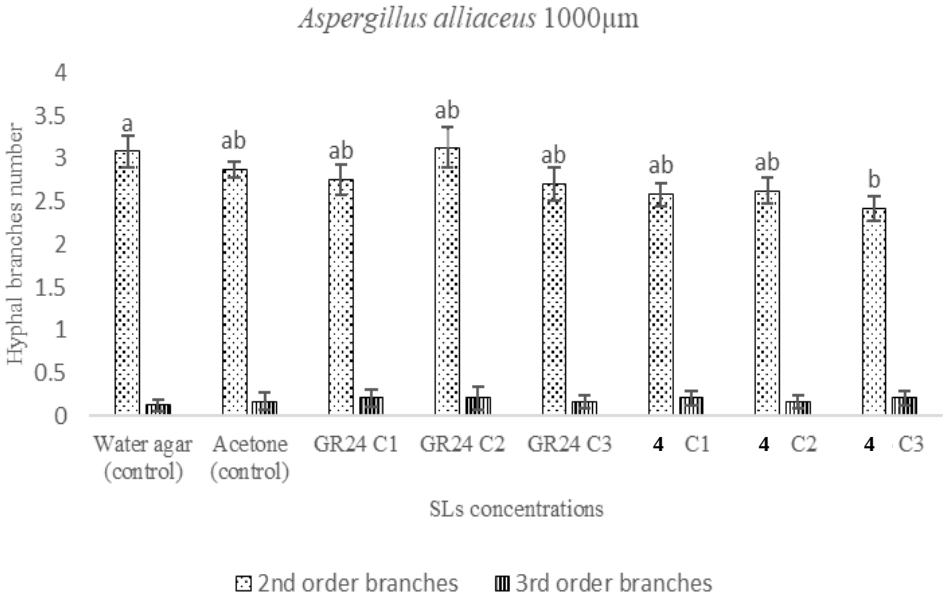

Fig. 10 – The influence of SLs on fungal hyphal branching for *Aspergillus alliaceus*. The total number was recorded on a total length of 1000 µm. The bars represent the standard errors. The values followed by the same letter do not differ significantly at $p < 0.05$.

In the case of 2nd order branches for *Aspergillus alliaceus* the groups were not homogeneous in variance with respect to Levene statistic (p-value = 0.026) showing that for different treatments the number of counted hyphae had different distributions. However, the tests were done in triplicates and it was not considered enough to dismiss an analysis by ANOVA. The contrast test yielded some difference with respect to the 2nd order hyphae between the treatments and the blank groups. ANOVA yielded a low, marginally significant difference (p-value = 0.053, F = 2.609) with a significant difference for the contrast test (p-value = 0.017; t = -2.933) (Table 2).

Tukey's post hoc test (Figure 10) showed marginally significant differences only between treatment **4**-C3 and two other groups: the water blank treatment (p-value = 0.096) and GR24-C2 (p-value = 0.067).

Parasitic plants use strigolactones as a cue for plant root presence.[55] The strigolactones were considered as being "a cry for help in the rhizosphere", *i.e.*, exo-signals used by sessile plants to recruit mutualistic organisms.[56] In the case of volatiles acting as a plant "cry for help" for recruitment of the herbivores insect predators are also used as a cue by the parasitoids of herbivores insect predators.[57] Our hypothesis was, that according to the molecular logic of the below-ground communication, pathogens of the parasitic plant should use the same cue to locate their host. Our finding indicates that, at tested concentrations, **4** does not significantly influence the branching of *A. alliaceus*, a pathogen of the parasitic weeds that responds to SL mimic **4**.[45] Other bioassays (*e.g.*, chemotactic movement) are needed to evaluate strigolactone mimics and analog effects on fungal pathogens of parasitic plants.

The tested strigolactones have an effect on the biofilm formation by a nodulation enhancer. *Paenibacillus graminis* FL400. Strigolactones analogs were proven to modulate quorum sensing related features of rhizobia (*Sinorhizobium meliloti*), such as swarming mobility.[58] Recently it was proven that strigolactones influence *quorum sensing* (QS) in *Vibrio cholerae*.[59]

Our experiment demonstrates that strigolactone promote biofilm formation on sand particles by a nodulation enhancer, *P. graminis* FL400 (Figure 11). This suggests a multiple function of these endo- and exo-signals produced by plants, including one related to microbiome shaping.[60]

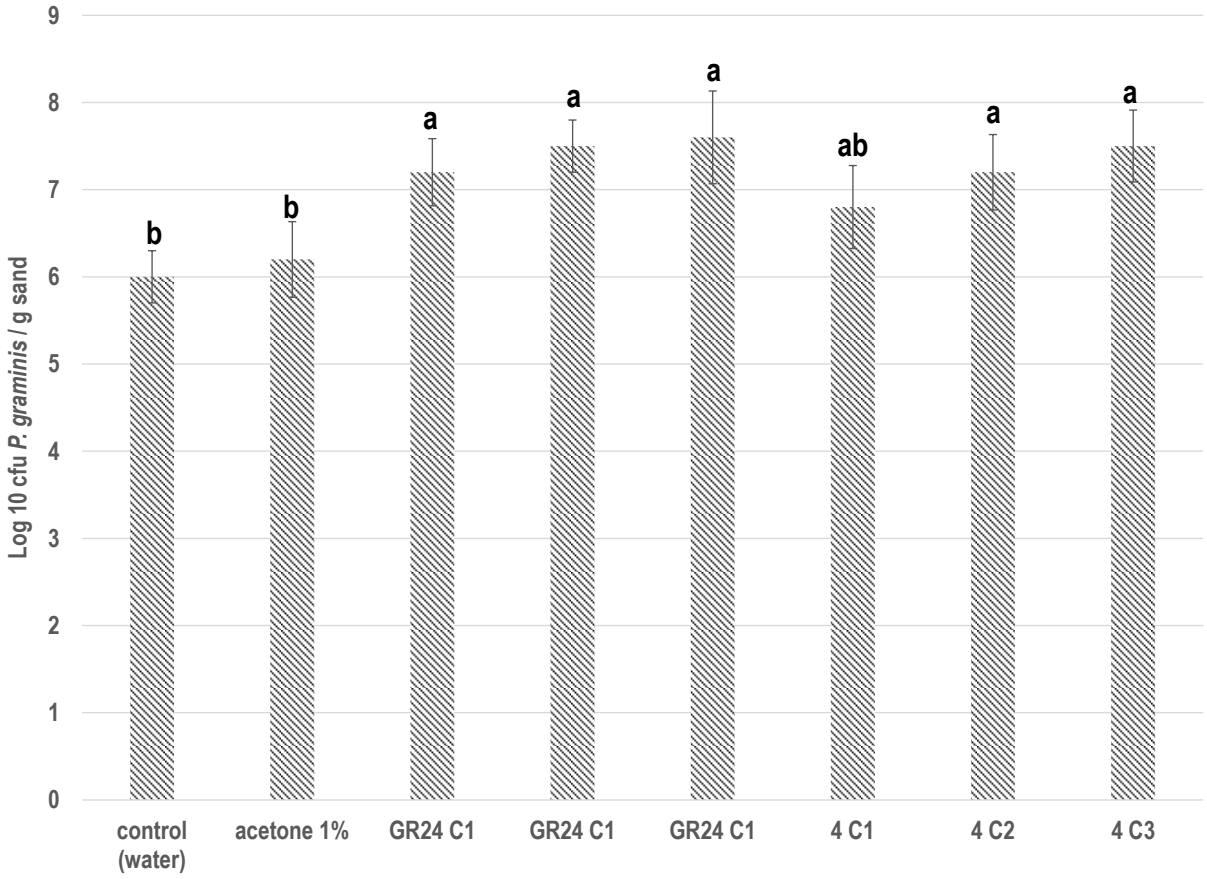

Fig. 11 – The influence of SLs on sand biofilm formation by *P. graminis*. The bars represent the standard errors. The values followed by the same letter does not differ significantly at $p < 0.05$.

EXPERIMENTAL

Materials and Methods

Melting points were determined on a Boetius apparatus and are uncorrected. The IR spectra were recorded on a Nicolet Impact 410 spectrometer, in KBr pellets. The NMR spectra analysis were recorded on a Bruker Avance III 400 spectrometer, operating at 400.1, 100.6 and 40.6 MHz for ^{1}H, ^{13}C and ^{15}N, respectively. The 1D and 2D spectra were recorded with a 5 mm multinuclear inverse detection z-gradient probe. 2D NMR correlation spectra (H-H COSY, H-C HSQC, H-C HMBC and H-N HMBC), were recorded with standard pulse sequences delivered by Bruker with TopSpin 2.1 PL6 spectrometer control and processing software. Chemical shifts are reported in δ units (ppm) and were referenced to the residual solvent signals (for $CDCl_3$ ^{1}H at 7.26 ppm and ^{13}C at 77.0 ppm). The ^{15}N chemical shift, obtained as projection from the indirectly detected H-N HMBC, is referenced to liquid ammonia (0.0 ppm) using nitromethane (380.2 ppm) as external standard. Exact mass of SL mimic **4** has been determined from high resolution MS spectrum recorded on a Bruker Maxis II QTOF spectrometer with electrospray ionization (ESI) in positive mode. Electronic absorption spectra were obtained on a UV-Vis spectrometer (SPECORD 200PLUS, Analytik Jena) in 10 mm path length cuvettes. The fluorescence spectra were recorded with a Perkin Elmer LS55 luminescence spectrometer using quartz cells of 10 mm optical path length. The solvents of spectrophotometric degree used in this work were toluene (PhMe), dichloromethane (DCM) and dimethylformamide (DMF) (Sigma-Aldrich). The fluorescence quantum yield (Φ) was determined in dilute solutions (A <0.1) at the excitation wavelength corresponding to the maximum of the absorption bands on a FLS980 spectrometer (Edinburgh Instruments) using an integrating sphere.

All reagents and solvents were purchased from Sigma-Aldrich and used without supplementary purification. *Aspergillus alliaceus* CBS 563.65 was purchased from CBS-KNAW (Westerdijk Fungal Biodiversity Institute), Utrecht, The Netherlands. The *Paenibacillus graminis* FL400 was a gift from Research-Development Institute for Plant Protection, Bucharest. The reference compound GR24 was purchased from Stichting Chemiefonds Paddepoel (Stg CfP), Malden, The Netherlands.

Note on the naming of the compound in the experimental section: in the first part we used the name of the compound according to IUPAC rules. However, in the experimental part we choose to numbering the furanone ring with the 1,8-naphthalinimide unit attached to C-5, as the most of SL-analogs and mimics are usually numbered.

Synthesis of 2-(4-methyl-5-oxo-2,5-dihydro-furan-2-yloxy)-benzo[*de*]isoquinoline-1,3-dione (4, alternative name 3-Methyl-5-(benzo[*de*]isoquinoline-1,3-dione-2-yloxy)-5H-furan-2-one)

To a suspension of 2.38 g (12 mmol) of 1,8-naphthalic anhydride **1** in 30 mL dioxane, 1.04 g (15 mmol mmol) of hydroxylamine hydrochloride and 2.07 g (15 mmol) of anh.

K_2CO_3 were added and the reaction mixture was heated at reflux temperature for 8 hours. The reaction mixture was poured on 100 g of crushed ice and neutralized with HCl 5%. The formed solid was filtered off and washed on the filter with water and acetone to give 2.36 g (92% yield) *N*-hydroxy-1,8-naphthalimide **2**, m.p. 285-287°C which was used directly into the next step. To a solution of 2.13 g (10 mmol) *N*-hydroxy-1,8-naphthalimide **2** in 15 mL DMF were added anh. K_2CO_3 (1.52 g, 11 mmol) and crude 5-bromo-3-methyl-5*H*-furan-2-one **3** (2.21 g, 12.5 mmol) under stirring at room temperature. The stirring was continued at room temperature for the next 20 h. Then, the reaction mixture was poured into 80 mL water and extracted with CH_2Cl_2 (3 x 75 mL). The combined extracts were washed with an equal volume of water and dried over anh. Na_2SO_4. The solvent was partly removed under reduced pressure, the residue was chromatographed on a SiO_2-packed column eluting with EtOAc:hexane 25% and finally recrystallized to obtain the SL mimic **4**, as beige solid, 2.54 g yield 82 %, m.p. 236-238°C (acetone / MeOH).IR (KBr, $\nu_{C=O}$, cm^{-1}): 1789, 1726, 1688. ^{1}H NMR (CDCl3, γ, ppm): 2.02 (s, 3H, CH3), 6.48 (s, 1H, H-5), 7.18 (s, 1H, H-4), 7.79 (t, 2H, J = 7.8 Hz, H-5'), 8.26 (d, 2H, J = 8.1 Hz, H-6'), 8.64 (d, 2H, J = 7.3 Hz, H-4'). ^{13}C NMR (CDCl3, γ, ppm): 10.8 (CH3), 103.2 (CH-5), 122.5 (2 x C-3'a), 127.1 (2 x CH-5'), 127.5 (C-9'b), 131.8 (C-6'a), 132.1 (2 x CH-4'), 134.9 (2 x CH-6'), 136.0 (C-3), 139.9 (CH-4), 160.8 (2 x CO-1',3'), 170.7 (CO-2). ^{15}N NMR (CDCl3, δ, ppm): 223.1 ppm. The IR, ^{1}H and ^{13}C NMR spectra confirmed the structure of final reaction compound **4**.[45] HRMS-ESI (m/z): $[M+Na]^+$ for $C_{17}H_{11}NO_5Na$, calcd. 332.0529, found 332.05218.

Biological Activity Tests

We tested the effect of strigolactone mimic **4** on *Aspergillus alliaceus*, a pathogen of the parasitic plant from the *Orobanche Cumana* and the nodulation enhancers, *Paenibacillus graminis* FL400. The effects on the fungal pathogen of parasitic plant was tested according to slightly modified method from our previous paper related to strigolactone mimics.[45] Briefly, the inoculated Petri dishes were kept at 28ºC for 3 days. After 3 days, the developed fungal colonies were observed, and the Petri dishes were examined using a Leica DM 1000 LED (Leica Microsystems, Wetzlar, Germany) microscope provided with a digital camera ICC50W and images of the fungal colonies were captured on the 3rd day. The number of hyphal branches of different orders, from second (2º) till the maximum observed was recorded of each primary branch, moving back from the end of the youngest hyphal tip. Observations were focused on the arrangement and number of the hyphae.

We modified the sand attachment assay to estimate the strigolactone's ability to influence *in-situ* biofilm formation by a strain of nodulation enhancer *Paenibacillus graminis* FL400.[61] Briefly, *P. graminis* cells were grown to OD_{600} = 2.0 ($1x10^8$ cells/mL) in a low-nutrient peptone medium. The medium consisted of 2 g/L meat peptone, 5 g/L NaCl, and 5g/L K_2HPO_4 (Scharlab, Barcelona, Spain). The pH was adjusted to 7.0. Bacteria were then aseptically centrifuged, washed with sterile phosphate saline buffer, and resuspended to OD600 = 0.2 ($1x10^7$ cells/mL) in the same medium. Five hundred µl of sterile sand were placed in the wells of a 24-well Costar 3526 polystyrene (PS) dish (Corning Incorporated, Corning, NY, US) and was inoculated with 500 µl of cells or with the same volume of culture medium only. The dish was then incubated at 28ºC, and the cells were harvested at different time points. A volume of 100 µl of sand and liquid was removed by using a pipette fitted with a wide-bore tip and transferred to a pre-weighed microcentrifuge tube. All traces of liquid culture were removed by pipetting, and only the sand and tube were weighed. One-half of the sand samples were washed aseptically with 10 mM $MgSO_4$. To each sample, washed or otherwise, 150 mL of fresh 10 mM $MgSO_4$ were added, and the tubes were vortexed extensively to dissociate cells from the sand particles. The liquid containing the dislodged cells was serially diluted and plated on a selective medium for obtaining CFUs. The CFUs were normalized to the amount of sand weighed. The experiments were done in low-nutrient peptone medium and low nutrient peptone medium supplemented with strigolactone analog GR24 and strigolactone mimic SL 4. Three concentrations, 10^{-8} µM, 10^{-7} µM, and10^{-6} µM, were used. Also, the growing medium was supplemented with acetone (up to 1%), the solvent used for the GR24 and SL 4. Statistical analysis was performed using IBM® SPSS® Statistics, version 26. The experiments were made twice with three replicates in each and the presented data are from one of them.

CONCLUSIONS

Photophysical and biological properties of 2-(4-methyl-5-oxo-2,5-dihydro-furan-2-yloxy)-benzo [*de*]isoquinoline-1,3-dione, a strigolactone mimic which contain in its molecule the 1,8-naphthalimide ring connected by an ether link to the bioactive 3-methyl-furan-2-one unit, have been investigated. This strigolactone mimic shown promising fluorescent properties and proved to be active in promotion of the biofilm formation in nodulation enhancing bacteria. The interesting fluorescent and biologic properties of this compound prompted us to design and to synthesize fluorescent SL mimics in order to exploit them in bioimaging investigations.

Acknowledgement. Financial support through NO Grants 2014-2021, under Project RO-NO-2019-540 STIM 4$^+$, Contract No. 14⁄2020, is acknowledged. Access to research infrastructure developed in the "Petru Poni" Institute of Macromolecular Chemistry through the European Social Fund for Regional Development, Competitiveness Operational Programme Axis 1, Project InoMatPol (ID P_36_570, Contract 142/10.10.2016, cod MySMIS: 107464) is also gratefully acknowledged.

REFERENCES

1. C. E. Cook, L. P. Whichard, B. Turner, M. E. Wall and G. H. Egley, *Science*, **1966**, *154*, 1189–1190.
2. C. E. Cook, P. Coggon, A. T. McPhail, M. E. Wall, L. P. Whichard, G. H. Egley and P. A. Luhan, *J. Am. Chem. Soc.*, **1972**, *94*, 6198–6199.
3. E. M. Magnus and B. Zwanenburg, *J. Agric. Food Chem.*,**1992**, *40*, 1066–1070.

4. R. Matusova, K. Rani, F. W. A. Verstappen, M. C. R. Franssen, M. H. Beale and H. J. Bouwmeester, *Plant Physiol.*, **2005**, *139*, 920–934.
5. K. Akiyama and H. Hayashi, *Ann. Bot.*, **2006**, *97*, 925–931.
6. K. Yoneyama, X. Xie, K. Yoneyama and Y. Takeuchi, *Pest. Manag. Sci.*,**2009**, *65*, 467–470.
7. B. Zwanenburg, A. S. Mwakaboko, A. Reizelman, G. Anilkumar and D. Sethumadhavan, *Pest. Manag. Sci*., **2009**, 65, 478–491.
8. K. Akiyama, K. Matsuzaki and H. Hayashi, *Nature*, **2005**, *435*, 824–827.
9. H. J. Bouwmeester, C. Roux, J. A. Lopez-Raez and G. Becard, *Trends Plant Sci.*, **2007**, *12*, 224–230.
10. X. Xie, K. Yoneyama and K. Yoneyama, *Annu. Rev. Phytopathol.*, **2010**, *48*, 93–117.
11. K. Akiyama, S. Ogasawara, S. Ito and H. Hayashi, *Plant Cell. Physiol.*, **2010**, *51*, 1104–1117.
12. V. Gomez-Roldan, S. Fermas, P. B. Brewer, V. Puech-Pages, E. A. Dun, J.-P. Pillot, F. Letisse, R. Matusova, S. Danoun, J. C. Portais, et al., *Nature*, **2008**, 455, 189–194.
13. M. Umehara, A. Hanada, S. Yoshida, K. Akiyama, T. Arite, N. Takeda-Kamiya, H. Magome, Y. Kamiya, K. Shirasu, K. Yoneyama, et al., *Nature*, **2008**, 455, 195–200.
14. H. Koltai, E. Dor, J. Hershenhorn, D. M. Joel, S. Weininger, S. Lekalla, H. Shealtiel, C. Bhattacharya, E. Eliahu, N. Resnicket al., *J. Plant Growth Regul*., **2010**, *29*, 129–136.
15. Y. Kapulnik, P.-M. Delaux, N. Resnick, E. Mayzlish-Gati, S. Wininger, C. Bhattacharya, D. Séjalon-Delmas, J.-P. Combier, G. Bécard, E. Belausov, et al., *Planta*, **2011**, 233, 209–216.
16. H. Koltai, *New Phytol*., **2011**, *190*, 545–549.
17. C. Ruyter-Spira, W. Kohlen, T. Charnikhova, A. van Zeijl, L. van Bezouwen, N. de Ruijter, C. Cardoso, J. A. Lopez-Raez, R. Matusova, R. Bours, et al., *Plant Physiol.*, **2011**, *155*, 721–734.
18. F.-D. Boyer, A. de Saint Germain, J.-P. Pillot, J.-B. Pouvreau, V. C. Chen, S. Ramos, A. Stevenin, P. Simier, P. Delavault, J.-M. Beau et al., *Plant Physiol.*, **2012**, *159*, 1524–1544.
19. F.-D. Boyer, A. de Saint Germain, J.-B. Pouvreau, G. Clavé, J.-P. Pillot, A. Roux, A. Rasmussen, S. Depuydt, D. Lauressergues, N. Freidit Frey et al., *Mol. Plant*, **2014**, *7*, 675–690.
20. E. Dor, D. M. Joel, Y. Kapulnik, H. Koltai and J. Hershenhorn, *Planta*, **2011**, *234*, 419–427.
21. M. Umehara, A. Hanada, H. Magome, N. Takeda-Kamiya and S. Yamaguchi, *Plant Cell Physiol*, **2010**, *51*, 1118–1126.
22. W. Kohlen, T. Charnikhova, Q. Liu, R. Bours, M. A. Domagalska, S. Beguerie, F. Verstappen, O. Leyser, H. Bouwmeester and C. Ruyter-Spira, *Plant Physiol*, **2011**, *155*, 974–987.
23. C. V. Ha, M. A. Leyva-González, Y. Osakabe, U. T. Tran, R. Nishiyama, Y. Watanabe, M. Tanaka, M. Seki, S. Yamaguchi, N. V. Dong, et al. *Proc. Natl. Acad. Sci USA*, **2014**, *111*, 851–856.
24. E. L. Decker, A. Alder, S. Hunn, J. Ferguson, M. T. Lehtonen, B. Scheler, K. L. Kerres, G. Wiedemann, V. Safavi-Rizi, S. Nordzieke et al., *New Phytol*, **2017**, *216*, 455–468.
25. Y. Wang and H. J. Bouwmeester, *J. Experim. Botany*, **2018**, *69*, 2219–2230.
26. H. Koltai and C. Prandi (eds.), Strigolactones - Biology and Applications. Springer International Publishing, 2019, pp. 163-195. https://doi.org/10.1007/978-3-030-12153-2.
27. B. Zwanenburg, S. ĆavarZeljković and T. Pospíšil, *Pest Management Sci*., **2016**, *72* (*1*), 15–29; 637.
28. Y. Kondo, E. Tadokoro, M. Matsuura, K. Iwasaki, Y. Sugimoto, H. Miyake, H. Takikawa and M. Sasaki, *Biosci. Biotechnol. Biochem.*, **2007**, *71*, 2781–2786.
29. M. Lachia, H. C. Wolf, P. J. M. Jung, C. Screpanti and A. De Mesmaeker, *Bioorg. Med. Chem. Lett.* **2015**, *25*, 2184–2188.
30. A. Besserer, V. Puech-Pages, P. Kiefer, V. Gomez-Roldan, A. Jauneau, S. Roy, J.-C. Portais, C. Roux, G. Becard and N. Sejalon-Delmas, *PLoS Biol*., **2006**, *4*, 1239–1247.
31. B. Zwanenburg, T. Pospíšil and S. Ćavar Zeljković, *Planta*, **2016**, *243*, 1311–1326.
32. A. W. Johnson, G. Gowada, A. Hassanali, J. Knox, S. Monaco, Z. Razavi and G. Rosebery, *J. Chem. Soc., Perkin Trans. 1*, **1981**, 1734-1743.
33. E. M. Mangnus and B. Zwanenburg, *J. Agric. Food Chem.*, **1992**, *40*, 697–700.
34. E. M. Mangnus, F. J. Dommerholt, R. L. P. De Jong and B. Zwanenburg, *J. Agric. Food Chem.* **1992**, *40*, 1230–1235.
35. G. H. L. Nefkens, J. W. J. F. Thuring, M. F. M. Beenakkers and B. Zwanenburg, *J. Agric. Food Chem.* **1997**, *45*, 2273–2277.
36. A. S. Mwakaboko and B. Zwanenburg, *Bioorg. Med. Chem.*, **2011**, *19*, 5006–5011.
37. A. S. Mwakaboko and B. Zwanenburg, *Plant Cell Physiol.*, **2011**, *52*, 699–715.
38. M. Lachia, P.M.J. Jung and A. De Mesmaeker, *Tetrahedron Lett.*, **2012**, *53*, 4514–4517.
39. K. Fukui, S. Ito, K. Ueno, S. Yamaguchi, J. Kyozuka and T. Asami, *Bioorg. Med. Chem.Lett.* **2011**, *21*, 4905-4908.
40. B. Zwanenburg and A. S. Mwakaboko, *Bioorg. Med. Chem.*, **2011**, *19*, 7394–7400.
41. B. Zwanenburg, S. K. Nayak, T. V. Charnikhova and H. J. Bouwmeester, *Bioorg. Med. Chem. Lett.*, **2013**, *23*, 5182-5186.
42. M. T. Waters, C. Gutjahr, T. Bennett and D. C. Nelson, *Ann. Rev. Plant Biol.*, **2017**, *68*, 291-322.
43. M. Dvorakova, P. Soudek and T. Vanek, *J. Nat. Prod*., **2017**, *80*, 1318-1327.
44. A. de Saint Germain, G. Clavé, M.-A. Badet-Denisot, J.-P. Pillot, D. Cornu, J.-P. Le Caer, M. Burger, F. Pelissier, P. Retailleau, C. Turnbull, S. Bonhomme, J. Chory, C. Rameau, F.-D. Boyer, *Nature Chem. Biol.*, **2016**, *12*, 787–794.
45. F. Oancea, E. Georgescu, R. Matusova, F. Georgescu, A. Nicolescu, I. Raut, M.-L. Jecu, M.-C. Vladulescu, L. Vladulescu and C. Deleanu, *Molecules*, **2017**, *22*, 961–975.
46. E. Georgescu, F. Georgescu, M. M. Popa, C. Draghici, L. Tarko and F. Dumitrascu, *ACS Comb. Sci.*, **2012**, *14*, 101–107.
47. A. Oancea, E. Georgescu, F. Georgescu, A. Nicolescu, E. I. Oprita, C. Tudora, L. Vladulescu, M. C. Vladulescu, F. Oancea and C. Deleanu, *Beil. J. Org. Chem.*, **2017**, *13*, 659–664.
48. E. Georgescu, A. Oancea, F. Georgescu, A. Nicolescu, E. I. Oprita, L. Vladulescu, M.-C.Vladulescu, F. Oancea, S. Shova and C. Deleanu, *PLoS One*, **2018**, *13*, e0198121. DOI: 10.1371/journal.pone.0198121.
49. G. Macalpine, R. Raphael, A. Shaw, A. Taylor and H. J. Wild, *J. Chem. Soc., Perkin Trans. 1*, **1976**, 410–416.
50. M. Korzec, K. Malarz, A. Mrozec-Wilczkiewicz, R. Rzycka-Korzec, E. Schab-Balcerzak and J. Polanski, *Spectrochim. Acta Part A: Mol. Biomol. Spectrosc*., **2020**, *238*, 118442–118454.

51. M. Van Overtveldt, L. Braem, S. Struk, A. M. Kaczmarek, F.-D. Boyer, R. Van Deun, K. Gevaert, S. Goormachtig, T. S. A. Heugebaert, and C. V. Stevens, *Plant J*., **2019**, *98*, 165–180.
52. C. Prandi, H. Rosso, B. Lace, E. G. Occhiato, A. Oppedisano, S. Tabasso, G. Alberto, and M. Blangetti, *Molec. Plant*, **2013**, *6*, 113–127.
53. M. Marzec, and P. Brewer, *Trends Plant Sci*., **2019**, *24*, 571–574.
54. M. Bürger, and J. Chory, *Trends Plant Sci.*, **2020**, *25*, 395–405.
55. B. Zwanenburg, A. S. Mwakaboko and C. Kannan, *Pest Management Sci.*,**2016**, *72*, 2016–2025.
56. J. A. López-Ráez, M. J. Pozo, and J. M. García-Garrido, *Botany*, **2011**, *89*, 513–522.
57. M. Dicke, and I. T. Baldwin, *Trends Plant Sci.*, **2010**, *15*, 167–175.
58. M. A. Peláez-Vico, L. Bernabéu-Roda, W. Kohlen, M. J. Soto, and J. A. López-Ráez, *Plant Sci.*, **2016**, *245*, 119–127.
59. C. Mozes, and M. M. Meijler, *ACS Chem. Biol.*, **2020**, *15*, 2055–2059.
60. B. Aquino, J. M. Bradley and S. Lumba, *Plant J.*, **2021** *105*, 322–334.
61. S. M. Hinsa, M. Espinosa-Urgel, J. L. Ramos and G. A. O'Toole, *Molec. Microb.*, **2003**, *49*, 905–918.